

UNEXPECTED RESULTS ON MICROWAVE WAVEGUIDE MODE TRANSMISSION MEASUREMENTS IN THE SPS BEAM PIPE

T. Kroyer^{1†}, F. Caspers, W. Höfle, J. M. Jimenez, J.-F. Malo, J. Tückmantel, CERN, Geneva, Switzerland
[†] TU Wien, Institute of Communications and Radio-Frequency Engineering

Abstract

In order to measure the electron cloud density, a microwave transmission measurement was set up over 30 m in the SPS beam pipe. The use of TE waveguide modes eliminates direct interaction with the highly relativistic beam. An electron cloud present in the beam pipe should lead to a small phase shift of the CW microwave signal. Since this phase shift is modulated by the bunch revolution frequency, it translates to a phase modulation which can be measured. However, defying all expectations, a huge beam-induced signal attenuation was found which cannot be understood by current electron cloud models. This attenuation showed erratic memory effects in the order of microseconds after the passage of a batch or single bunch. Both effects are present for a wide range of microwave signal frequencies and beam parameters. Models to possibly explain this effect are discussed.

INTRODUCTION

The initial goal of the measurements presented in this paper was the determination of the electron cloud density in the SPS beam pipe. For this purpose TE type waveguide modes were sent along 30 m of the SPS close to the BA2 access point. In this section are mainly dipoles with one quadrupole between. Initially a measurement over 1000 m had been planned, but the waveguide mode attenuation turned out to be much higher than expected.

Using TE modes rules out any direct interaction with a highly relativistic beam in the center of the beam pipe. However close to inhomogeneities like beam pipe cross-section changes or pumping ports some interaction might occur. The impact of direct beam interactions of this kind should remain small due to a very low transit-time factor. Such signals should appear in very limited frequency bands, and by a simple measurement without active microwave signal it can be checked whether the direct beam interaction can be neglected or not.

Other effects, not directly beam-induced, have to be attributed to an electron plasma in the beam pipe. A direct interaction between the electromagnetic wave and ions can be ruled out on account of the greater inertia of the ions.

Measurement set-up

Figure 1 shows the measurement set-up used. A CW signal in the range of 3 GHz is generated on the surface and

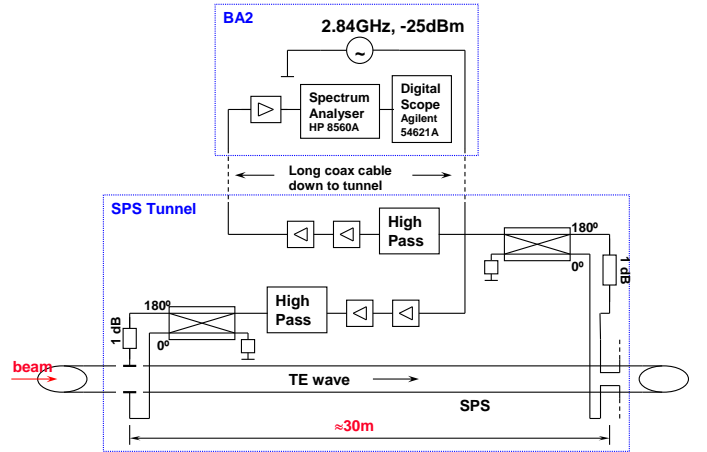


Figure 1: Measurement set-up

sent down into the tunnel. Due to the considerable cable attenuation a 70 dB amplification in the tunnel was necessary. Then the signal crosses a high pass filter protecting the amplifiers against low frequency beam signals. This high pass was realised by a short section of S-band waveguide which cuts off all frequencies below 2 GHz. A hybrid splits the signal in two components having opposite phases. Feeding these signals into a pick-up consisting of two electrodes on the longer sides of the beam pipe excites a TE mode. Since the electrodes are on the vertical symmetry axis of the beam pipe, the only possible TE modes are of $TE_{2n+1,2m}$ type, with non-negative integers n and m . The first two modes are therefore the TE_{10} and the TE_{30} , with cut-off frequencies of about 1 GHz and 3 GHz, respectively.

To stop charge building up on the pick-up electrodes, which could drive the amplifiers into saturation, 1dB attenuators were used as DC returns. Unfortunately there were no dedicated pick-ups for the frequency range over 1 GHz at hand. As an alternative, a home-made wide band button pair was installed for the left pick-up in Fig. 1 while at the other end the upstream port of a stripline monitor was used. Since these pick-ups were never foreseen for waveguide mode excitation, it is not surprising that their coupling efficiency is not optimum. In Fig. 2 the hardware transfer function (HTF) is shown. The HTF is the response of the entire measurement assembly in transmission mode, including amplifiers and the beam pipe with no beam in the SPS. The red

¹tom.kroyer@cern.ch

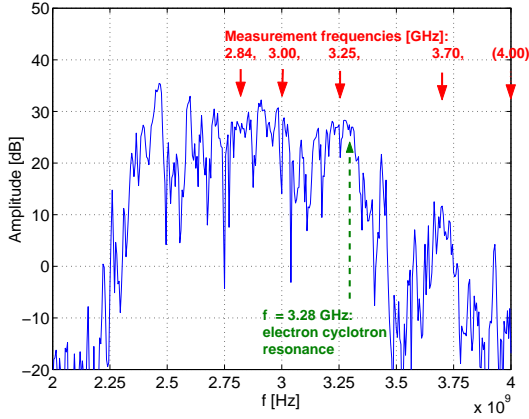


Figure 2: The hardware transfer function of the measurement set-up in Fig. 1. Between 2.3 and 3.25 GHz the transmission through the entire system is reasonably high. Note that the absolute amplitude is not relevant, since the amplifier chains are included in the measurement.

arrows indicate the frequencies chosen for later observations.

After having traversed the beam pipe, the signal passes through the DC return, the hybrid, the high pass filter, the amplification and the long cable to the surface. Following further amplification by 35 or 70 dB the signal is displayed on a spectrum analyser (SPA). To circumvent the problem caused by the maximum SPA frequency of 2.9 GHz, the signal was transposed to a lower frequency band by an external mixer and an additional local oscillator.

Initial plans for doing measurements between two SPS access points over a distance of 1000 m were abandoned since the attenuation turned out to be too high. Bad coupling efficiency of the pick-ups and an additional transmission attenuation by cross-section changes appear to be the reason for this.

Expected Results

The maximum density for a classical electron cloud is in the order of $\rho_e \approx 10^{12} \text{ m}^{-3}$ [3]. For an electromagnetic wave propagating in an unmagnetized cold plasma, the phase shift over a length L is given by [1]

$$\Delta\phi = -\frac{1}{2} \frac{\omega_p^2}{\omega c} L \quad (1)$$

with the plasma frequency $\omega_p = \sqrt{4\pi\rho_e r_e c^2}$, the classical electron radius r_e and the speed of light c . Over 30 m an electron cloud density of 10^{12} m^{-3} should lead to a phase shift of about 0.6° for a frequency of 2.5 GHz^2 . The electron cloud appears when a batch or single bunch passes and decays afterwards with a time constant in the order

²A similar effect limits the precision of GPS. In the ionosphere the maximum plasma density is roughly 10^{12} m^{-3} . After propagation over 500 km a phase delay of 1 m can be observed, corresponding to a phase shift of 4° per meter [2]. The GPS frequencies (1.575 GHz for the L1 downlink) are in the order of those used in the SPS measurement.

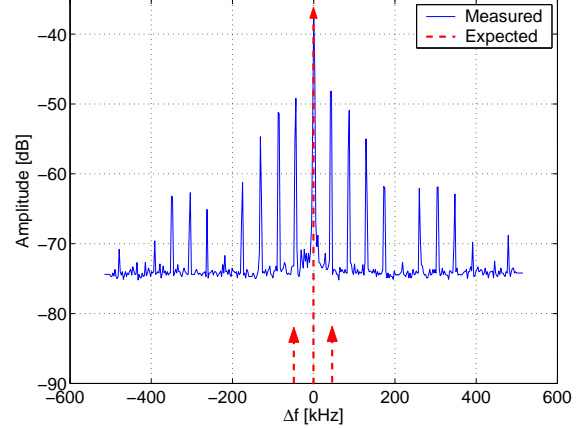


Figure 3: The measured modulation spectrum compared to a sine FM with $\beta = 0.01$.

of 100 ns [3]. Therefore the phase shift is translated into a phase modulation, with the SPS revolution frequency of $f_{\text{rev}} = 43 \text{ kHz}$ being the modulation frequency. The phase shift $\Delta\phi$ in [rad] corresponds to the modulation index β . For $\Delta\phi = 0.6^\circ$ we get $\beta = 0.0105 \ll 1$, which implies a narrow band frequency modulation. The expected spectrum consists of the carrier with two side bands spaced at $\pm f_{\text{rev}}$. The side band amplitude should be $\beta/2 = 46 \text{ dB}$ below the carrier.

THE MEASUREMENT

As can be seen in figure 3, a broad spectrum was found. Similar spectra were observed for all the excitation frequencies used (see Fig. 2), except for operation at 3.25 GHz. At this frequency the spectrum turned out to be asymmetric, which should be due to the nearby electron cyclotron resonance. The cyclotron frequency $f_b = \omega_b/2\pi$ is given by [1]

$$\omega_b = \frac{eB_0}{m} \quad (2)$$

where e is the elementary charge, B_0 the static magnetic field and m the mass of the particle. Applying equation 2 to electrons with the magnetic field during injection $B_0 = 0.117 \text{ T}$ yields $f_b = 3.275 \text{ GHz}$. Close to the cyclotron resonance, the ordinary modulation, which can be observed in a wide frequency band and the modulation due to cyclotron resonance are superposed. As a result, an asymmetric spectrum can be seen, which points toward a superposition of AM and FM.

It cannot be judged from Fig. 3 alone whether the spectrum comes from an AM or a wide band FM. However, it appears that there is only one dominating modulation, since the spectrum is symmetric, except for measurements near the electron cyclotron resonance. As will be pointed out in the next section, time domain considerations showed that the modulation found is nearly entirely AM. Conversely, the spectrum close to the electron cyclotron frequency can

be explained as a superposition of this AM with an FM due to the cyclotron resonance. In the following we shift our focus to time domain measurements. The initial concept of measuring a faint phase modulation by observing tiny side bands was abandoned for the time being.

Time domain measurements

It is difficult to interpret the data at hand just by looking at the spectrum as shown in Fig. 3. A much more convenient way is to observe the variation of the carrier in time domain plotting the CW transmission as a function of time. This was done by connecting the video output of the analog spectrum analyser to a digital scope, as shown in the schematic view of the measurement set-up (Fig. 1). The rise time of the entire system is limited by the resolution bandwidth of the SPA. Using the maximum resolution bandwidth of 2 MHz, a rise time of about

$$t_r = \frac{1}{3 \cdot 2 \text{ MHz}} \approx 170 \text{ ns} \quad (3)$$

was obtained. Since the available resolution bandwidth is larger than the modulated spectrum, the total signal energy is captured. For a pure FM the signal energy should not vary with time. However, strong fluctuations in signal amplitude have been found, which suggests that we are dealing with an absorption amplitude modulation. This “absorption” can be due to power dissipation as well as to reflection.

Preparatory measurements. In a first step the CW transmission over a full SPS machine cycle was measured without beam. This corresponds to evaluating the variation of the hardware transfer function with time. At one frequency, namely $f = 3.00 \text{ GHz}$, a magnetic field dependant amplitude and phase shift was observed. This seems to be due to ferromagnetic material in the beam pipe exposed to the fringe field of the bending magnets. A very likely candidate is the NiCr layer coated ceramic tubes used for microwave absorption in the pumping ports. Since this modulation is very slow compared to the SPS revolution frequency and its maximum amplitude excursion does not exceed 7 dB, this effect was neglected in the following. As a second check, the beam induced signals were measured. Figure 4 shows data for two batches in the SPS. The beam gaps can be well distinguished between the batches. During the passage of the beam, the induced signal rises up to 10 dB out of the noise floor. Since the beam is highly relativistic it takes only 100 ns for the 30 m long measurement section, which is smaller than the rise time of the system.

Longitudinal beam profile. The trace in Fig. 5 was taken during a machine development session. It is worth noting that the signal *decreases* when there is beam. In fact, during the passage of a batch, the signal gets attenuated by more than 30 dB and disappears in the noise floor. As in Figure 4 the noise background is situated around -45 dB. Of course the absolute numbers

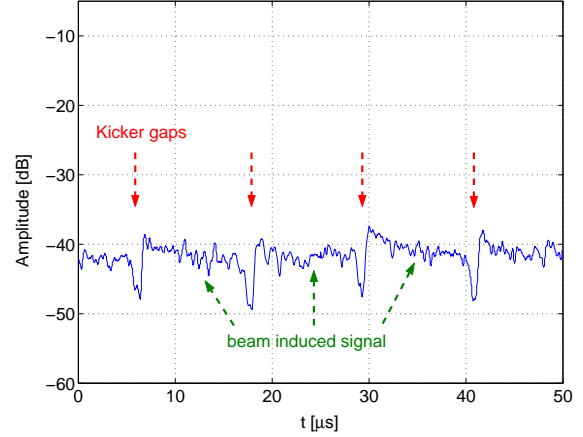


Figure 4: The beam induced signal (pick-up signal) for two SPS batches with the microwave carrier off. Around every $11 \mu\text{s}$ the kicker gap can be seen as a little notch.

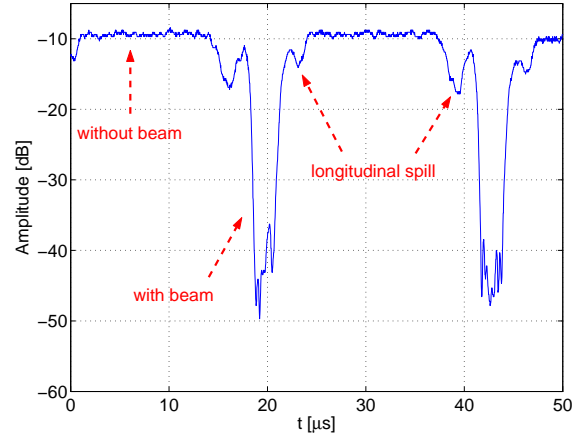


Figure 5: Data taken during a machine development session, with the same measurement and display settings as in Fig. 4. The microwave signal is attenuated by more than 30 dB with beam.

are irrelevant, since they depend on the amplifiers and on the SPA settings. For the given set-up the dynamic range (noise floor to maximum signal) is 35 dB. Obviously this is not enough to see what happens in the center of a batch. The main limiting factor for the dynamic range is the output power of the last amplifier before coupling to the beam pipe. The measured signal attenuation between the two pick-ups is roughly 70 dB. It is caused mainly by the pick-up insertion losses, with additional losses coming from cross-section changes, interconnects and pumping ports equipped with absorbing material. Modifications in the set-up aiming at increasing the dynamic range are under discussion. The most promising options are the use of a high power amplifier and to perform the measurements over shorter lengths, such as 10 m.

In Fig. 5, on both sides of each batch smaller notches can be seen which come from particles that are not captured in

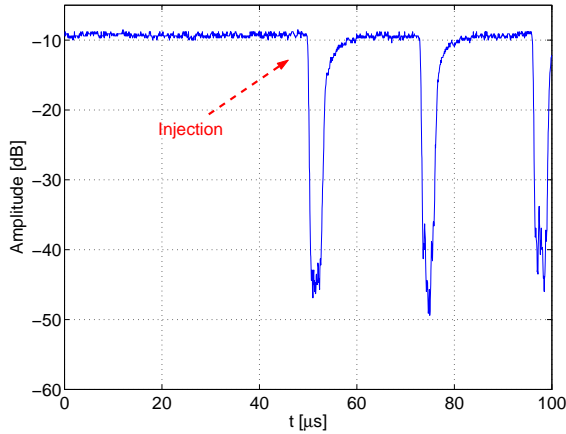


Figure 6: The first turns of one LHC type batch.

the RF buckets. This pattern corresponds very well to data from beam monitors.

Memory effects. Since the entire project was carried out parasitically, that is, without dedicated beam time, we had to accept what was available in terms of beam type, intensity, etc. Many measurements were performed using essentially three different types of beam:

- LHC type: 25 ns bunch spacing, 26 GeV/c at injection, acceleration up to 450 GeV/c.
- FT (Fixed Target) type: 5 ns bunch spacing, 14 GeV/c at injection, accelerated up to 450 GeV/c.
- Single bunch beam.

Fig. 6 shows a measurement with LHC type beam with one batch. The data acquisition was triggered on injection to exclude memory effects. Already in the first turn it can be seen that the rising edge of the signal is slightly rounded off. Even stronger “tails” like this can be seen in Fig. 7. Instead of going right back to the initial signal level after the passage of the beam, the signal climbs only slowly. Fits with exponential functions for the tails yielded time constants in the region of $1.5 \mu\text{s}$. The first, steeper parts of the tails have smaller time constants around $1 \mu\text{s}$, while the later parts can be fitted best with exponentials having time constants around $2 \mu\text{s}$. A cross-check with the steepest slope in the plot gave a time constant of roughly 150 ns, in good agreement with the calculated system rise time.

It is very interesting to note that the tails occur in a very random manner. No periodicity could be found in the tail pattern. A sample of 22 turns in Fig. 8 illustrates this behaviour. The maximum record length on the digital scope at hand was not more than 2000 samples, which made a subsequent statistical data analysis difficult. For future measurements the use of a scope with longer record length is considered, which should allow a better examination of the tail fluctuations.

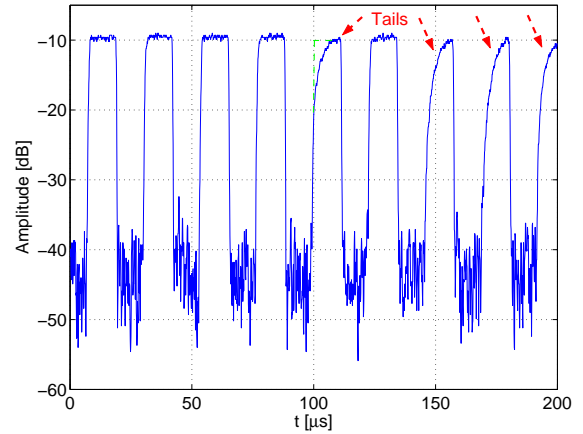


Figure 7: Characteristic tails, observed with an FT type beam.

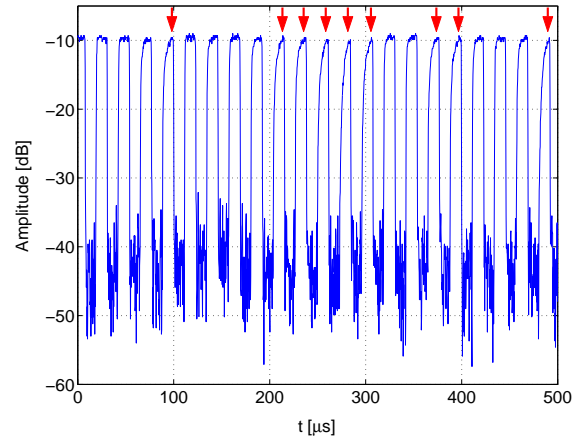


Figure 8: A longer observation period reveals the random occurrence of the tails. For clarity, strong tails have been marked with an arrow.

For high intensity beams like those considered before, the signal vanished immediately in the noise. Fig. 9 depicts data from a low intensity beam ($< 10^{10} \text{ p}^+$). In this case a distinct build-up time can be observed which occurs at every turn. However, at least in the present data, no tails could be found.

Variation of beam and measurement parameters.

Single bunch beams constitute a particularly interesting case. The measurements were carried out with 4.13 ns long bunches of low intensity (10^{10} p^+). Transmission data taken at three different CW frequencies showed the familiar picture: wildly fluctuating tails (Fig. 10). We tried to find three representative traces among the collected data. Please note that the measurements at different frequencies were not made simultaneously. Traces above 3.25 GHz were found to have a rather poor SNR and were thus omitted. It appears that at lower excitation frequencies the tails are more pronounced, but more data are necessary to confirm this.

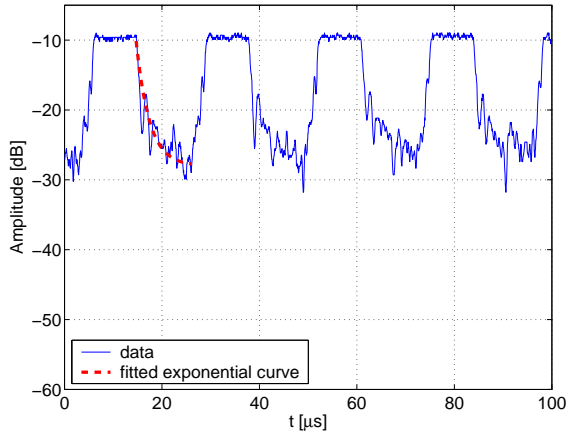


Figure 9: With a low intensity beam a build-up time could be observed.

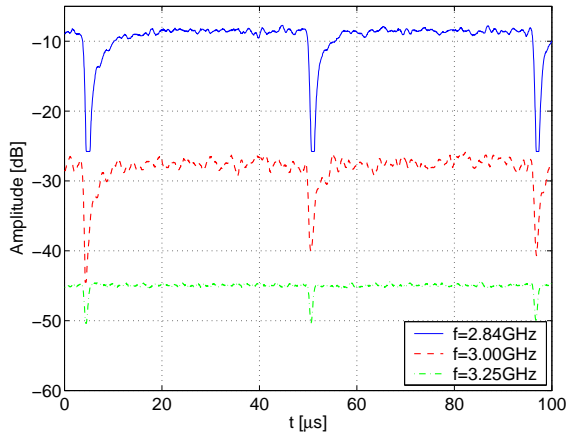


Figure 10: Tails observed for a single bunch beam. Please note that the three traces were *not* taken simultaneously and that, as always, the absolute amplitude is not relevant.

Several complementary measurements were performed to check the dependence of the tails on important parameters. In addition to different beam types, including single bunch beams, the following parameters were varied:

- CW frequency. As for the single bunch beam (Fig: 10) measurements at 2.84, 3.0, 3.25 GHz and other frequencies were performed.
- Beam intensity.
- Magnetic field. Several measurements were carried out at different instants of the machine cycle, especially at injection (0.117 T), during the ramping and on the flat top.
- Vacuum pressure. Since any kind of ionization effect should depend on vacuum pressure, it was varied between 3×10^{-8} and 1.3×10^{-7} Torr. A larger pressure increase would have required a major intervention and probably cost beam time.

None of these modifications lead to a visible change in the properties of the tails.

SUMMARY & DISCUSSION

We did not succeed in measuring the electron cloud density by means of the microwave transmission experiment presented. Instead two phenomena on the transmission signal were observed, (a) a strong amplitude modulation and (b) memory effects associated with the amplitude modulation, such as tails and build-up times of the order of μs . Both effects can not be explained by current electron cloud theories. Theory also suggests that direct beam interaction can be ruled out, a fact that was checked in preparatory measurements. Unlike the case of electron cloud formation, no distinct threshold has been found.

The AM in (a) could be explained by a high reflection coefficient from an electron plasma at cyclotron resonance. However, this would require - at least locally - charge densities beyond 10^{16} m^{-3} , which is in contradiction to today's understanding of electron clouds. The density of a classical electron cloud is roughly 10^{12} m^{-3} , which is four orders of magnitude lower.

Origin of the tails

Perhaps even more interesting are the memory effects that were found, in particular the tails. This effect may be linked to the mechanism causing the high attenuation during the passage of the beam, but it is not certain. Simulations show that electrons from electron clouds may form a so-called pinch when a bunch of positively charged particles passes. However they are cast against the beam pipe wall afterwards with time constants in the order of 100 ns [3]. This is far too fast to explain our observations. Secondary electrons bouncing off the walls like those forming electron clouds would drift long enough, but the charge densities are by far too small. Other effects like plasma-wakefield interactions in the fringe field of the magnets or close to inhomogeneities can be thought of, as well.

However, all those theories presented for the explanation of the memory effects encountered have two weak points in common. On the one hand they don't explain why tails appear for such a wide variety of beam parameters, magnetic fields, and CW frequencies. On the other they don't offer any hint on the randomness of the tails' occurrence.

The dust hypothesis

Another contribution to the observed effects could come from microparticles with diameters of the order of $1 \mu m$ in the beam line. It is commonly known that dust trapping was a major concern in electron machines [4]. In some cases trapped microparticles managed to stay in the beam line for several seconds. Of course this is not possible with protons and positive ions in the SPS, because in general

dust particles are positively charged.

However, dust particles could still get raised and cross the beam. Conducting microparticles usually stick to the walls due to electromagnetic interactions.

For positive beams, they are not supposed to come off the wall. On the other hand, for isolating particles it can be imagined that they get charged and hop off the wall. During the verification of ultra clean surfaces, isolating dust particles have been observed to jump back and forth between the tip of a scanning electron microscope and a metallic surface [5]. Some of the particles raised could cross the beam line. In this case, a plasma would form around the heated dust particle and get dragged along with the beam. First estimations showed that the plasma density could be comparable to the particle density in the beam. Therefore the slowly moving plasma ions would keep the plasma electrons confined in a small cylindrical region. The lifetime of ion plasmas in the beam pipe is in the order of $1\ \mu\text{s}$, which corresponds well to the observed rise times. The dust hypothesis is just a very tentative theory, but it allows an explanation of all the observations related to the tails - at least qualitatively. Dust raising should not be very sensitive to variation of parameters, and the randomness comes in naturally.

Things to do

Many ways of how to refine the measurements were discussed. Here we cite the most promising ones:

- Measurement with higher microwave power to increase the dynamic range
- Operation in reflection mode to check for scattered power
- Measurement in the opposite direction (against the beam) by swapping excitation and measurement pick-up
- Injection of small quantities of other gases to get a significant increase in vacuum pressure
- Injection of microparticles by mechanical vibrations of the beam pipe to check the dust hypothesis
- Installation of a scintillation counter to detect scattered particles
- Repetition of the experiment in another machine

ACKNOWLEDGEMENTS

We would like to thank Thomas Bohl and Frank Zimmermann for help and advice. Thanks to Flemming Pedersen for inspiring discussion, Trevor Linnecar for support and last but not least Noël Hilleret for the initial suggestions and helpful discussion.

REFERENCES

- [1] Heald, M. A. and Wharton, C. B., *Plasma Diagnostics with Microwaves*, Wiley, New York, 1965
- [2] Herring, T., *Modern Navigation*,
<http://bowie.mit.edu/tah/12.215>
- [3] Zimmermann, F., *Electron-cloud Simulations: An Update*, Chamomix, 2001
- [4] Kelly, D.R.C. *Dust in Accelerator Vacuum Systems*, Proceedings of the Particle Accelerator Conference, 1997, Vol.3, Iss., 12-16 May 1997 Pages: 3547-3551 Vol.3
- [5] *Private communication with E. Mahner*